Journal of Civil Structural Health Monitoring
https://doi.org/10.1007/s13349-024-00780-2

ORIGINAL PAPER

On the combined use of satellite and on-site information for monitoring anomalous trends in structures within cultural heritage sites

Melissa De Iuliis[1] · **Marianna Crognale**[1] · **Francesco Potenza**[2] · **Vincenzo Gattulli**[1]

Received: 26 March 2023 / Accepted: 6 February 2024

Abstract
Existing structures and infrastructures are exposed worldwide to different types of hazards during their service life, such as earthquakes or landslides, especially in countries characterized by high seismicity and hydrogeological risk, as Italy. Mitigation risk and safeguarding existing structures are tasks of great interest for structural engineering. Recently, advanced multi-temporal differential synthetic aperture radar interferometry (DInSAR) products have been used to monitor the evolution in time of ground movement that affects structures. This paper proposes a methodological approach to integrate DInSAR data, visualized in the GIS environment, with on-site measurements. DInSAR and terrestrial laser scanning (TLS) are purposely combined to facilitate the spatial interpretation of displacements affecting cultural heritage sites. An insight into the proposed approach is provided through the study of the Capitoline Museums in Rome (Italy) focusing on Marcus Aurelius Exedra, by exploiting the data archive (ascending and descending acquisitions) collected during the 2012–2020 time interval. Identifying possible critical situations for the analyzed structure is carried out through the analysis of DInSAR-based displacements time series and mean deformation velocity values. Ascending and descending data are combined to extract the components of ground motions and reveal the presence of predominant components in the vertical direction. This is also confirmed by comparing the "as-build" model (obtained from TLS) and the "as-design" model (obtained from the original technical drawing). Therefore, the DInSAR–TLS combination allows supporting structural health monitoring early warning procedures of structures.

Keywords Structural health monitoring · DInSAR measurements · Terrestrial laser scanning · Early warning · Displacement time series

1 Introduction

The built environment has recently been subjected to different natural phenomena and extreme events highlighting how buildings, infrastructures, and architectural heritage structures are highly vulnerable. Therefore, the interest in approaches that examine buildings, particularly those with historical value, has been strengthened to assess the structural behavior, ensure the safety of constructions, and enforce the prioritization of monitoring and conservation policies to ensure sustainable conservations. Structural health monitoring (SHM) and assessment techniques are paramount to verifying the residual capacity of existing buildings and infrastructures that could reach or even overcome their service life [1, 2]. Traditional SHM applications require many sensors, such as accelerometers; they can be time-consuming data collection, expensive, labor intensive,

✉ Melissa De Iuliis
melissa.deiuliis@uniroma1.it

Marianna Crognale
marianna.crognale@uniroma1.it

Francesco Potenza
francesco.potenza@unich.it

Vincenzo Gattulli
vincenzo.gattulli@uniroma1.it

[1] Department of Structural and Geotechnical Engineering, Sapienza University of Rome, Via Eudossiana 18, 00184 Rome, Italy

[2] Department of Engineering and Geology, University "G. D'Annunzio" of Chieti-Pescara, Viale Pindaro 42, 65127 Pescara, Italy

Published online: 19 March 2024

and dangerous [3]. To address such limitations, especially where artistic and archeological heritage is extensive and developed, advanced non-destructive techniques are necessary for SHM applications. Among the available non-invasive SHM technologies, remote sensing techniques can be a valid option to provide helpful information to assist management decisions and safety evaluations while minimizing the effects of disturbances on the structure functionality. Although the advantages and potentialities of applying satellite remote sensing for urban applications were first investigated in 1985 by Forster [4], the employment of this approach for SHM is recent, and interferometric synthetic aperture radar (InSAR) data analysis approaches are under continuous development [5]. The ground displacement time series based on the analysis of differential interferometric synthetic aperture radar (DInSAR) data is considered a suitable approach for the structural assessments, particularly when it is combined with information about the geology of the area and the geometry of the structure under monitoring. DInSAR allows mapping and measuring deformation phenomena with a convenient cost/benefit ratio compared to traditional topographic techniques [6]. In recent years, DInSAR techniques have been widely used to analyze Earth surface displacement processes such as seismic events, landslides, volcano unrests, and subsidence [7–9]. Numerous applications of DInSAR satellite data for monitoring ground deformations can be found in the literature. In some studies, the processing of satellite SAR has allowed obtaining of ground deformation measurements and thus to detect of superficial deformations caused by natural and anthropic phenomena on single buildings [10–14], and extended areas [15, 16]. Similarly, terrestrial SAR interferometry was applied to study the effects of vertical settlements related to subsidence or excavations in the urban area of Rome (Italy) [17–19]. Bozzano et al. [20] performed satellite SAR to infer the recent deformational history of the "Vittoriano" monument in Rome (Italy) using medium- and high-resolution SAR images acquired in double orbital geometry and covering the last two decades. A structural monitoring and assessment methodology, including SAR approaches, was proposed by Talledo et al. [21]. In their work, the method was applied to the complex building of San Michele in Rome (Italy) to assess the structural behavior of the structure. Arangio et al. [22] integrated the results of a DInSAR analysis with an intermediate semi-empirical model to analyze three buildings located in the southern part of Rome (Italy). Bonano et al. [23] extended the Satellite BAseline Subset (SBAS) approach to generate deformation time series at full spatial resolution from long sequences of European Remote Sensing (ERS) and Environmental Satellite (ENVISAT) SAR data. Their approach was validated by processing two ERS/ENVISAT data sets relevant to the Napoli Bay Area (Italy), and the Murge region (Italy) acquired in 1992–2007. Satellite data have also been used to assess external actions not related to subsidence. For instance, Bayramov et al. [24] used satellite radar remote sensing to evaluate quantitatively ground deformation risks and movement trends for the onshore petroleum and gas industry. Although the use of SAR techniques in civil engineering has been improved, exploiting such approaches in the monitoring and structural assessment of structures withing cultural heritage sites is still an open issue.

The complexity of constructions within historical sites with irregular geometry, inhomogeneous materials, variable morphology, alterations, and damages, poses numerous challenges in the digital modeling and simulation of structural behavior. Terrestrial laser scanning (TLS) has been widely applied for periodic deformation monitoring of structures in recent years. TLS is a ground-based technique that automatically collects the 3D spatial coordinates of many points of objects in a very short period. The main advantage of the monitoring by TLS is its full surface 3D representation; other advantages of TLS include non-contact long-range measurements, a high degree of automation, and intensive sampling capability. TLS has been introduced for deformation monitoring of several applications in the fields of architecture, civil engineering, manufactory, and archaeology [25–27].

In this research scenario, the objective of this paper is to present a methodological approach based on the application of satellite data for detecting anomalous displacement trends of existing buildings placed in cultural heritage sites that could need further and more in-depth investigations. Thereafter, the retrieved information is combined with on-site information obtained from 3D terrestrial laser scanning (TLS) to support and validate the information, and consequently the interpretation of data acquired by DInSAR technique to provide a useful monitoring procedure tool that helps deeply investigating the actual conditions of the existing structures.

The methodology presented has been applied to analyze displacement trends at two different scales: at global scale accounting for the entire complex of Capitoline Museums in the city of Rome (Italy) as a whole (global analysis); at local scale focusing only on the Marcus Aurelius Exedra structure (local analysis). This is useful for the identification of the relative stability among the constructions in the area. DInSAR deformation data, obtained from the processing of ascending and descending COSMO-SkyMed images for 2012–2020, have been used to detect ground movements. Furthermore, on-site measurements conducted for the local analysis through the 3D TLS procedure have allowed the designing of an "as-built" model to determine the actual geometrical conditions of the analyzed structure and to identify the elements of the structure that are subjected to the displacements obtained from the DInSAR results. Compared to

traditional surveying techniques, TLS provides accurate and dense information in a rapid and non-invasive manner [28]. The combined use of TLS and SAR systems has been poorly studied, and the literature is limited to forest fire [29, 30] and vegetation estimation [31]. Therefore, combining TLS and SAR results is considered an important part of the presented work. Although further research is necessary to improve the accuracy of DInSAR in measuring small structural deformation phenomena, the presented results can help evaluate the structural condition of buildings within cultural heritage sites and demonstrate how DInSAR information could drive the application of traditional on-site experimental investigations in an optimal way. The paper is structured as follows: Sect. 2 is devoted to describing the proposed methodology for the preliminary structural assessment based on the joint exploitation of the satellite DInSAR data techniques and on-site measurements highlighting the key aspects and specific features of the DInSAR approach. In Sect. 3, the application of the proposed methodology to the case study, imaged by the COSMO-SkyMed SAR constellation from ascending and descending orbits during the 2012–2020 time interval, is presented, and the interpretation of the displacements for the identification of possible damage scenario is discussed. Moreover, in this section, on-site measurements to capture data about the actual condition of the analyzed structure are also described. Section 4 discusses the proposed methodology highlighting how the integration between DInSAR and on-site inspection results can effectively optimize the assessment of the structural health. Finally, conclusive remarks are drawn in Sect. 5.

2 Data and methods

This section describes the methodology proposed for the preliminary structural assessment of constructions based on the GIS integration of DInSAR measurements and 3D laser scanning. In particular, the methodology employs the DInSAR products (i.e., deformation time series and mean displacement velocity maps) computed by processing large full-resolution SAR datasets acquired from two different perspectives, ascending (ASC) and descending (DES) orbits, by the COSMO SkyMed (CSK) satellite constellation in the period from March 2012 to March 2020. Surface displacements relevant to the investigated area are carried out by processing SAR data stacks through the multi-temporal DInSAR technique, known as SBAS methods [32, 33]. Some post-processing techniques using two DInSAR datasets (ASC and DES) are described to extract two components of the actual deformation pattern affecting the examined structure. Finally, considerations on the structural assessment of the construction can be provided by combining the so-elaborated DInSAR-derived products with on-site information and measurements. The proposed methodology can be summarized as follows (see Fig. 1).

- Step 1: *SAR data processing* (identified by blue color). In the first step, deformation measurements along the radar sensor line of sight (LOS, i.e., the direction joining the sensor with the target on the ground) are computed, such as displacement time series and the corresponding mean velocity for each coherent measure point, named Persistent Scatterer (PS). Furthermore, velocity maps of the investigated area along the LOS are retrieved.
- Step 2: *Post-processing* (identified by grey color). This step aims at determining the two deformation components along the vertical and horizontal directions through interpolation strategies.
- Step 3: *On-site information* (identified by orange color). The third step deals with the geometrical identification of the investigated structure through the 3D scanning process to define the precise geometrical condition of the structure.
- Step 4: *Deformation assessment* (identified by yellow color). The methodology's final step is performed by combining information from DInSAR measurements with those derived from on-site data to identify possible critical situations which need in-depth investigation.

2.1 Overview of the SBAS-DInSAR approach

In this section, the main characteristics of both the SBAS-DInSAR approach and the exploited CSK datasets applied to compute the displacement time series and their mean deformation velocities are briefly described.

The SBAS methodology is the well-established advanced DInSAR technique that provides information on the temporal and spatial patterns of the radar-detected LOS-projected displacement components through the generation of deformation time series and mean velocity maps with sub-centimetric accuracy [32, 33]. The SBAS approach is based on using many SAR images acquired by satellite sensors over the analyzed area and during a given time to generate a multi-temporal sequence of differential interferograms, defining the phase differences between two SAR images. The multi-temporal sequence of differential interferograms is carried out by selecting the interferometric SAR data pairs that have a slight separation (i.e., perpendicular baseline) between the acquisition orbits and a low time interval between the involved SAR data (i.e., temporal baseline), which makes it possible to minimize noise effects, known as decorrelation effects [34], affecting the generated interferograms and, as a result, to maximize the spatial density of the retrieved DInSAR measurements, corresponding to the derived coherent points that, as previously mentioned, are defined as Persistent

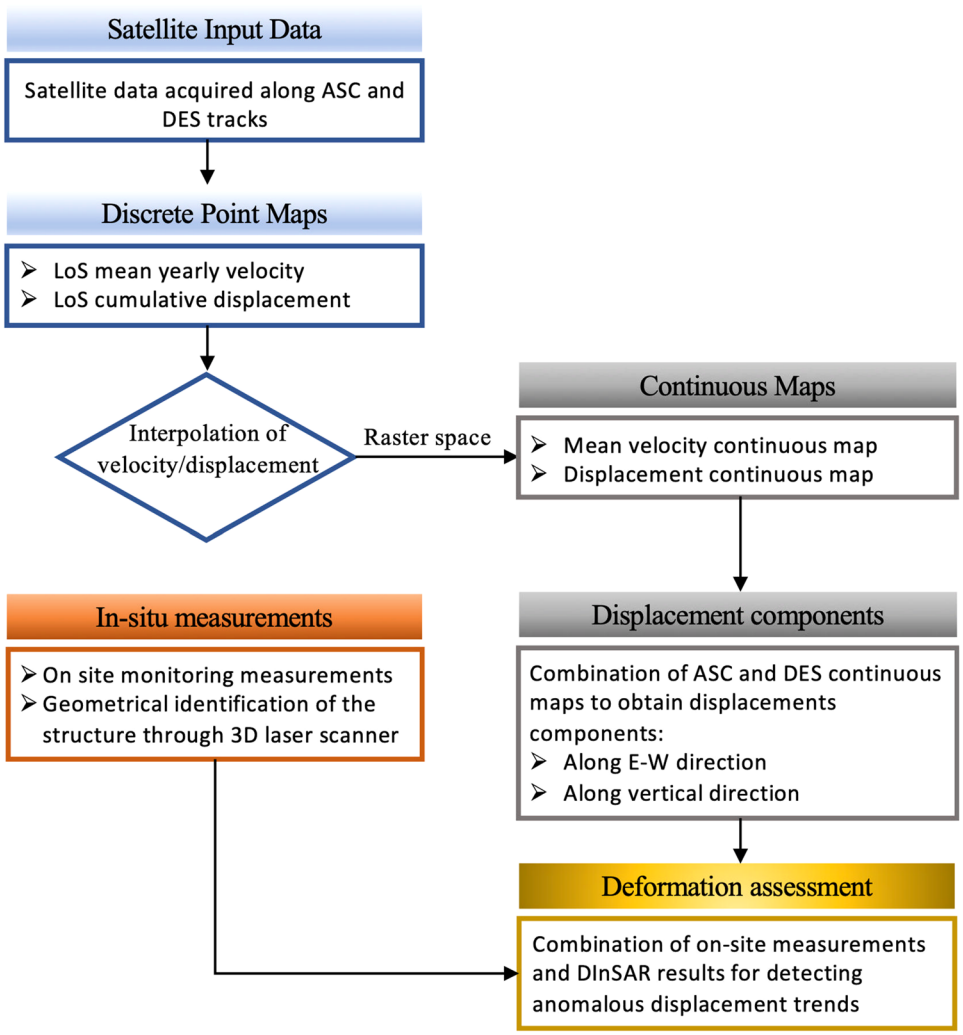

Fig. 1 Flowchart of the proposed methodology

Scatterers (PS). The accuracy of the obtained DInSAR products is about 1–2 mm/year for the mean deformation velocity information and 5–10 mm for the single deformation measurement [35, 36]. The main characteristic of the SBAS-DInSAR techniques is the ability to retrieve displacement time series and corresponding velocity maps at different spatial scales, i.e., regional (low-resolution analysis) and local scale (full-resolution analysis) analysis [36, 37]. While the first one allows investigating natural and anthropic deformation phenomena in large areas, the latter is particularly suitable for monitoring the deformation phenomena related to single buildings, infrastructures, or parts of them [38, 39]. This is accomplished by dealing with full-resolution differential interferograms, carried out from the single-look data with a typical spatial resolution of the sensor within the range of 3–10 m. In the following, the full-resolution SBAS-DInSAR approach applied to detect local scale deformation phenomena is described.

2.2 Measurements from satellite SAR interferometry

The full-resolution SBAS-DInSAR provides a large set of PSs relevant to the investigated area, for which measures of the displacements along the LOS direction are given within the analyzed time frame. Each PS is associated with an area of the surface whose dimensions are determined based on the resolution cell size of the processed SAR data. For each PS, the available information is: (i) the LOS displacement time series; the LOS mean deformation velocity; (iii) the geographical coordinates (latitude and longitude) and the altitude according to the global reference system; (iv) directional cosines of the LOS to identify the direction vector to which the displacement value refers; (v) and the temporal coherence, which is provided within the range [0, 1], to estimate the quality of the results on the pixels where the deformation time series are retrieved. Generally, the coherence threshold

is empirically set up by considering the characteristics of the analyzed dataset, such as the number of SAR acquisitions, the time interval, etc. For instance, a temporal coherence threshold of 0.35 can be considered while working with a CSK dataset that consists of about a hundred SAR images acquired over an urban area in a decade time interval [21]. As previously mentioned, radar images of the same area can be obtained from two perspectives ASC and DES. Thus, the proper combination of ASC and DES SAR acquisitions in different time frames over the same area, usually provided as ASCII text files, allows retrieving the components of the real deformation pattern, i.e., the vertical (V), the East–West (E–W), and the North–South (N–S) components of the displacement measurements. It is worth highlighting that since the ASC and DES satellite orbits are quasi polar, i.e., nearly perpendicular to the N–S direction, it is impossible to detect the N–S component with considerable accuracy. Indeed, it can be assumed that a deformation component along the N–S direction has a low influence on the LOS deformation values due to the low sensitivity when retrieving the N–S deformation component, which is around 5% [18]. To trace the components of the real displacement D_E and D_V information known from the satellite measure, i.e., the displacement D_{LOS} and the angles θ_E and θ_V must be used. Note that θ_E and θ_V are, respectively, the angles between the LOS and the three directions of the reference system (see Fig. 2).

Since the displacement measured along the LOS is computed as the sum of the projections on the LOS of the three cartesian components of the real displacement, it is possible to write two equations for both ascending and descending orbits that express the projection of the

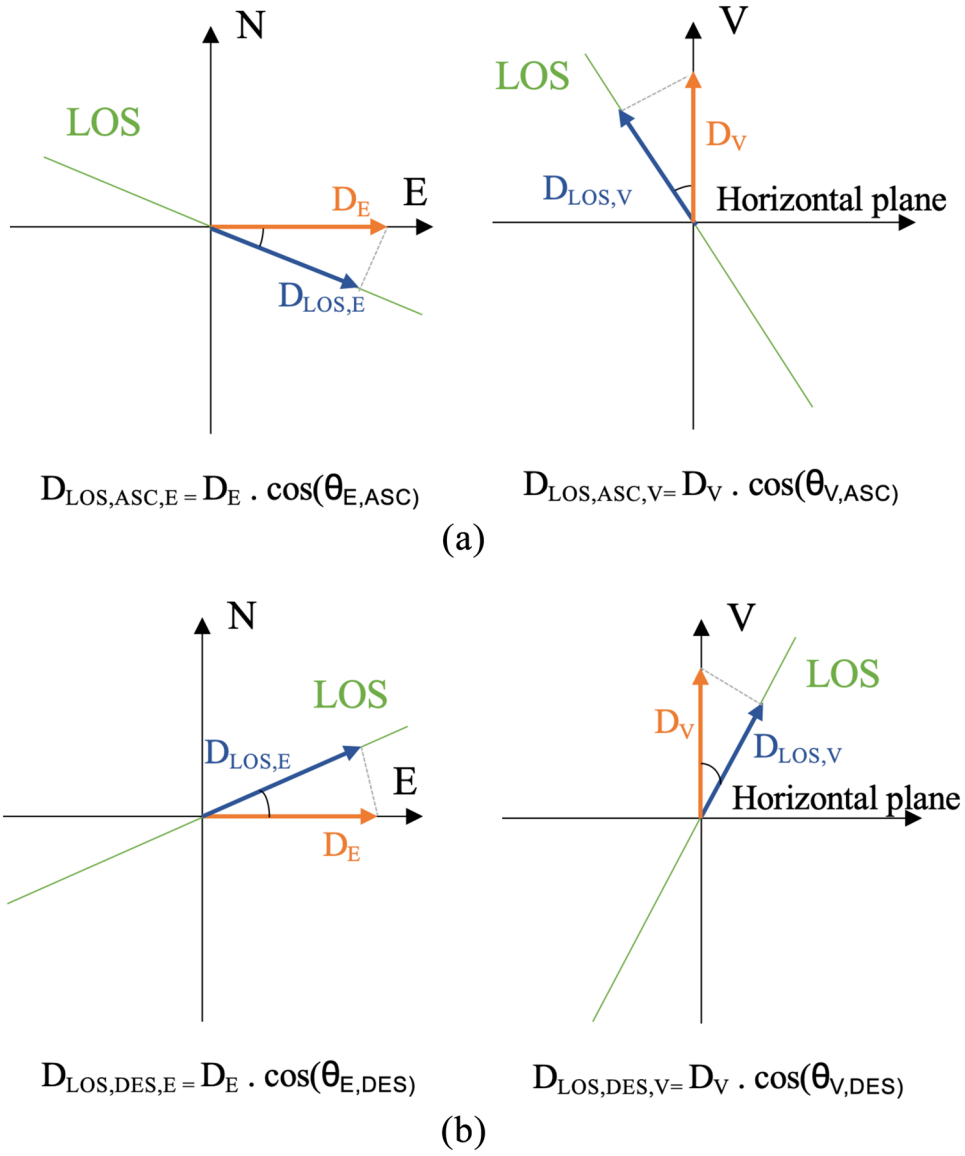

Fig. 2 Projections on the ascending (**a**) and descending (**b**) LOS of the components of the real displacement vector D_{LOS}

cartesian components of the real displacement on the two LOS directions (not coinciding with each other).

$$D_{\mathrm{LOS,ASC}} = D_{\mathrm{E-W}} \cdot \cos(\theta_{\mathrm{E,ASC}}) + D_{\mathrm{V}} \cdot \cos(\theta_{\mathrm{V,ASC}}),$$
$$D_{\mathrm{LOS,DES}} = D_{\mathrm{E-W}} \cdot \cos(\theta_{\mathrm{E,DES}}) + D_{\mathrm{V}} \cdot \cos(\theta_{\mathrm{V,DES}}). \quad (1)$$

To compute the vertical and horizontal components of the mean deformation velocity and displacement measured through the DInSAR analysis on the ground surface, a spatial resampling of both ASC and DES LOS velocity and displacement is implemented using the inverse distance weighted (IDW) interpolation method [40, 41], thus obtaining continuous maps of the mean LOS velocity and displacement, regarding the acquisition period. It is worth highlighting that having continuous maps helps immediately define the presence of zones affected by substantial velocity values along the two directions and zones characterized by a more stable behavior. Thus, the cell size of the IDW interpolation is set at 3m, according to the 3 X 3 m^2 resolution of COSMO-SkyMed products. In this way, the vertical and E–W components (associated with each point of the grid) can be computed with the system in Eq. (1). Note that Eq. (1) has been defined in terms of displacements, but it is extendable directly to computing the velocity components.

It is worth mentioning that interpolation techniques are valid under specific conditions of the disposition of the selected points. For instance, the use of interpolation procedures for defining velocity and displacement maps is not recommended where there is a low number of PSs [18].

3 Case study

To analyze the advantages of using the multi-temporal DInSAR approaches to support the structural health monitoring of structures, the historical complex of the Capitoline Museums in Rome (Italy) focusing on the Marcus Aurelius Exedra has been selected as a case study. The Capitoline Museums are the main civic museum of the city of Rome. The historical seat is constituted by the Palazzo dei Conservatori and the Palazzo Nuovo, both located on the Piazza del Campidoglio (Capitoline Hill). The new Hall of the Capitoline Museums, also called the hall of Marcus Aurelius, located at the ancient site of Giardino Romano (Roman Garden), displays the original equestrian statue of the Roman emperor of the second century AD (see Fig. 3a, b). The project was entrusted to Carlo Aymonino, one of the most important Italian architects of the last century, and it represents a prestigious piece of modern architecture within the ambit of the Municipal Museum complex that links the historic part of Palazzo dei Conservatori to those parts of the museum that have been more recently constructed. The large and bright hall was built in an open area that historically marked the

Fig. 3 Location of Capitoline Museums and Marcus Aurelius Exedra (from Google maps) (**a**) and internal view of the Marcus Aurelius Exedra (**b**)

boundary between the properties of the Conservators and the Caffarellis [42].

3.1 DInSAR analysis and displacement assessment

The interferometric products used in this work related to two sets of SAR images collected from ASC and DES orbits by the sensors of the Italian CSK constellation were provided by the Italian Space Agency (ASI) and processed by IREA-CNR through SBAS-DInSAR technique. The images were acquired through the standard Stripmap mode with Horizontal–Horizontal (HH) polarization and a ground spatial resolution of about 3 m in both azimuths (along-track) and range (cross-track) directions. The identified datasets comprise 129 ascending and 107 descending single-look complex (SLC) acquisitions collected from March 2012 to March 2020. The average look angles of the scene center are of about 34° and 29° for ASC and DES, respectively. The other characteristics of the exploited CSK datasets are listed in Table 1.

Table 1 Main characteristics of the exploited CSK datasets

	Ascending	Descending
Wavelength	3.1 cm	3.1 cm
Acquisition mode	H-IMAGE	H-IMAGE
Average look angle	32°	29°
Spatial extension	40 km × 40 km	40 km × 40 km
Spatial resolution	3 m × 3 m	3 m × 3 m
Beam-ID	H4-05	H4-03
Time interval	21/03/2012–11/03/2020	21/03/2012–11/03/2020
Number of acquisitions	129	107

IREA-CNR provided datasheets including different unique pixel identifiers for which several parameters are identified: latitude, longitude, topography, mean deformation velocity, interferometric temporal coherence, components of Line of Sight (LOS) unit vector along the North, East, Vertical directions, and LOS displacement time series (TS). Figure 4 shows the LOS mean deformation velocity maps expressed in mm/year on orthophotos, obtained by independently processing the two ASC (Fig. 4a) and DES (Fig. 4b) datasets at the full spatial resolution scale in the period from 2012 to 2020. The two mean deformation velocity maps show a good PSs density within the analyzed area, where almost all the structures are detected. It is evident from the figure that low deformation values characterize both quadrants containing the investigated structure.

As evidenced by the statistical distributions of the data of each orbit in Fig. 5, almost all velocities are between −0.2 and 0.2 mm/year.

The statistical distributions have an average value of about −0.0035 mm/year, and they are asymmetric to the mean value (skewness < 0) and leptokurtic (kurtosis > 3). From a first observation on a territorial scale, there are no areas subject to particularly high mean deformation velocities. The available data were analyzed in a geographic information system (GIS) environment, which allows organizing and displaying data associated with a position on the Earth's surface, to display the measurement points on the investigated structure and analyze their displacement time series.

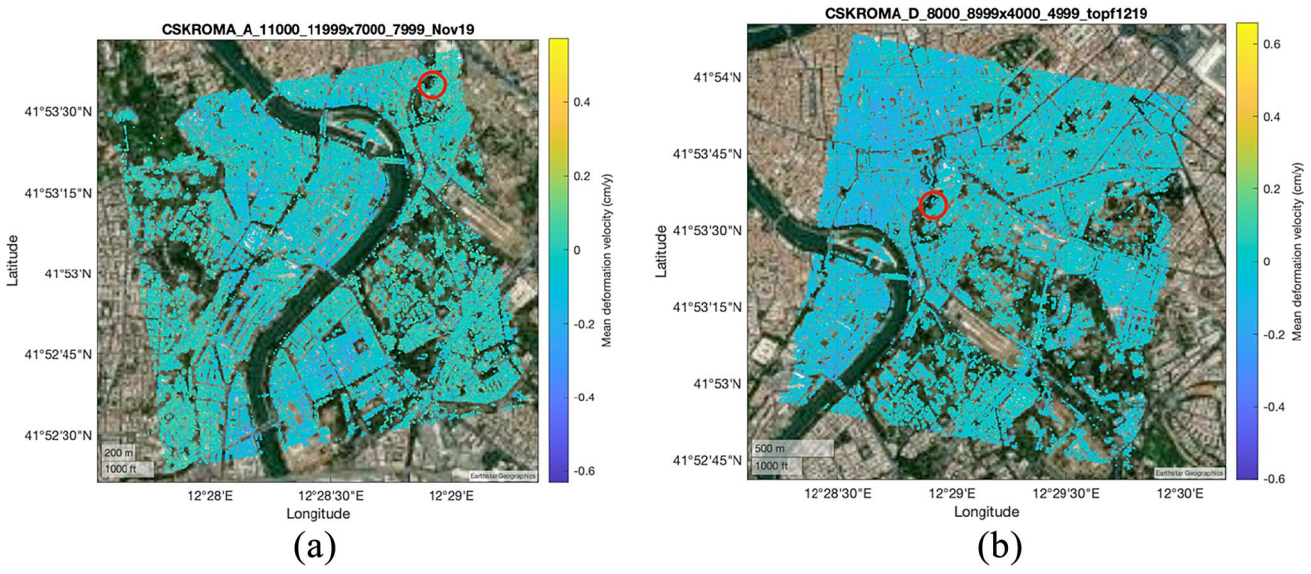

Fig. 4 View of the analyzed area with superimposed the LOS mean deformation velocity map for the identified PSs and different longitude and latitude coordinates. The red circle in both figures indicates the Marcus Aurelius Exedra of Capitoline Museums

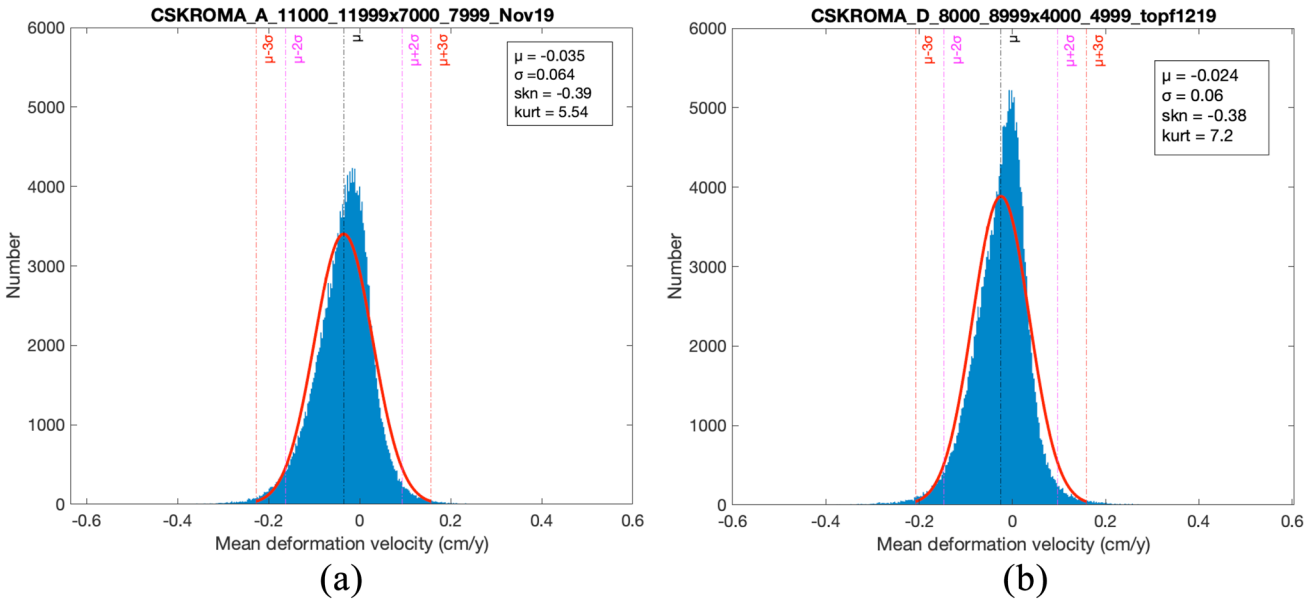

Fig. 5 Distribution of mean deformation velocities: ascending (**a**) and descending (**b**) orbit. In the figures, μ is the mean, σ is the standard deviation, *skn* is the skewness value, and *kurt* represents the kurtosis value

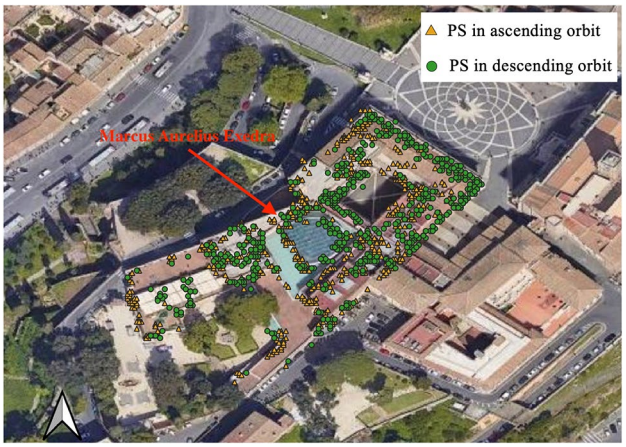

Fig. 6 PSs localization on Capitoline Museums, in ascending (yellow triangles) and descending (green circles) orbits, from QGIS

The localization of the PSs was obtained by converting the geodesic coordinates according to the reference ellipsoid WGS84 in cartesian coordinates, assuming the direction x coincident with that of the E–W direction. Limited to the area of Capitoline Museums, satellite data are available for both orbits. More precisely, it is possible to identify 734 PSs for the ascending and 726 for the descending orbit. The Marcus Aurelius Exedra consists of 58 PSs for the ascending orbit and 65 PSs for the descending orbit. The orthophoto representation denotes a good agreement between the positions of the satellite-detected scatterers on the building and the plan geometry (see Fig. 6).

Furthermore, the measured points were selected, and their displacement time series were analyzed. For example, Fig. 7 reports the displacement time series relating to the measured points on the Marcus Aurelius Exedra and associated with the ascending orbit. Since the descending orbit presents not-so-significant values of deformation velocities, it has been decided to neglect it. The time histories of the PSs belonging to the building show the presence of significant residual displacements at the end of the measurement period. In particular, the two PSs located in the eastern and northern part of the roof of the building (see Fig. 7a) exhibit high negative (i.e., moving away from the satellite, illustrated in red line) and positive (i.e., moving towards the satellite, illustrated in green line) deformation velocities, respectively. Figure 7b depicts the displacement time series of two points identified along the ascending LOS showing a certain regularity of the movement trend affected by annual temperature variations, i.e., downwards movements during autumn/winter season, and upwards movements during spring/summer season. Although the temperature has not been measured, it is certainly possible to assume a thermal excursion of at least 20°. The information coming by historical trends of the displacements helps identifying a certain seasonality movement that could be better recognize if a significant time window is investigated (e.g., seven or more years).

The vertical and E–W components of the displacement can be evaluated using the IDW interpolation method, as described in Sect. 2.2. The combination of maps carried out along the two tracks has allowed the detection of cumulated vertical and horizontal E–W

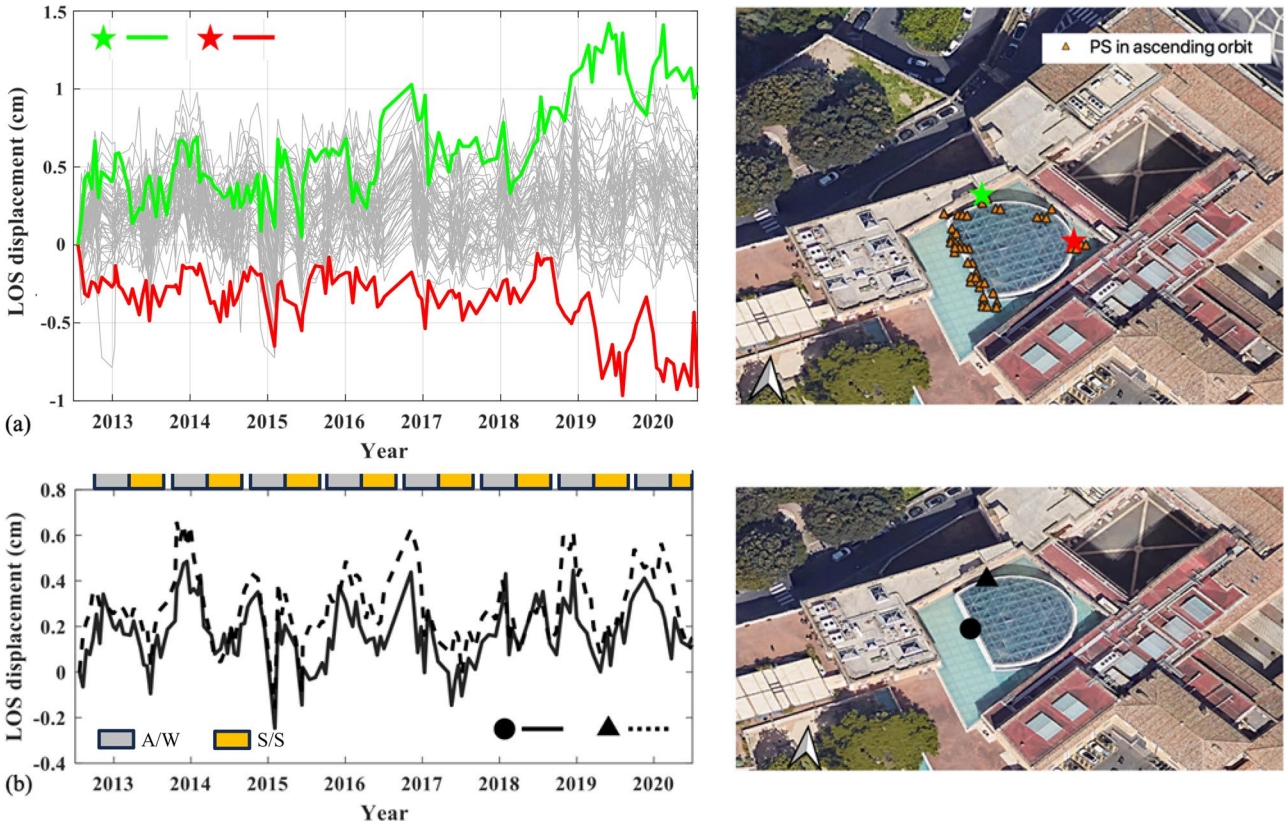

Fig. 7 Displacement time series of the analyzed points within the ascending orbit. The black curves are the interpolations of the measured trends (in red and in green) (**a**); displacement time series of two points showing the seasonality of the movements (**b**). In the images on the right are indicated the positions of the corresponding time histories highlighted in the left graphs. The grey and orange boxes in (**b**) represent the autumn/winter (A/W) and spring/summer (S/S) periods, respectively (color figure online)

movement components for each grid vertex. For convention, upwards and east-directed displacements have positive values, according to the reference system depicted in Fig. 2. The symbology used to represent the displacements along the two components, has graduated colors ranging from red (upwards and East-directed displacements, respectively) to blue (downwards and West-directed displacements, respectively). Green zones are characterized by stable behavior, not affected by displacements. The vertical and E–W components of the deformation velocity obtained by performing the analysis at global scale (Capitoline Museums) are illustrated in Fig. 8.

The analysis of the scenario of interest concludes that the structure is overall characterized by slight or negligible movements, indicating substantial stability. On the other hand, results indicate the presence of localized deformation. It is possible to identify the areas affected by movements downwards and towards the west direction—Tiber alluvial plain (represented by blue color) with velocities between 0.1 and 0.16 mm/year. Figure 8a shows that the northwest part of the structure is affected by upwards displacements with velocities between 0.122 and 0.172 mm/year. The true range of values for VV was − 0.112 mm/year to + 0.122 mm/year and VE − 0.158 to + 0.172 mm/year as listed in Table 2.

The results follow the studies conducted on the deformation trend that involves the historic center of Rome and the surrounding area in the last few years [43, 44]. Recent studies have claimed that displacements are mainly caused by subsidence or natural/human-induced deterioration processes experienced by archeological structures. Bozzano et al. [20] identified two different areas: the easter area, where the Capitoline Museums are located, is affected by slight or negligible movements downwards the Tiber alluvial plain, whereas the western region is affected by significant deformations and settlements caused by the subsidence of compressible soils (see Fig. 9).

Within all the observations conducted on the global scenario, particular attention was given to Marcus Aurelius Exedra. The same approach has been implemented

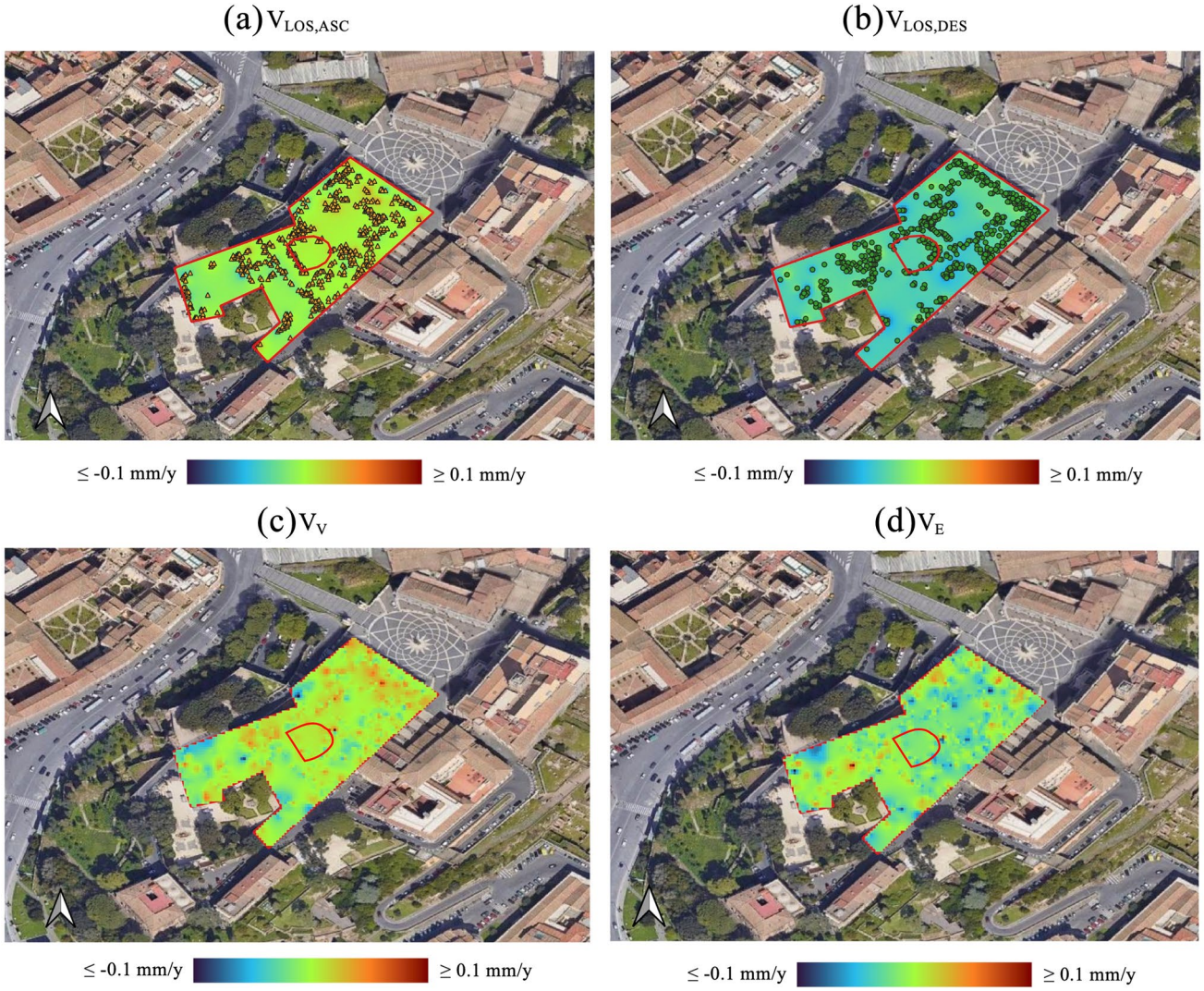

Fig. 8 Mean velocity maps of the Capitoline Museums (global scale): ASC (**a**) and DES (**b**) data, with IDW interpolation; vertical (**c**) and E–W (d) components of the mean velocity

to compute the vertical and E–W components of the deformation velocity and displacement at the local scale. Results are depicted in Figs. 10 and 11.

The true range of values for VV was − 0.076 mm/year to + 0.208 mm/year and VE − 0.417 to + 0.361 mm/year as listed in Table 3, and the true range of values for DV was − 2.147 cm to + 0.928 cm and DE − 0.032 cm to + 1.196 cm (see Table 3).

Table 2 Summary of min and max values of the vertical (VV) and horizontal (VE) deformation velocity during 2012–2020—Capitoline Museums

Value	VV (mm/year)	VE (mm/year)
Min (downwards/west)	− 0.112	− 0.158
Max (upwards/east)	0.122	0.172

3.2 On-site measurements: point cloud geometry reconstruction through 3D scanning

This subsection describes the terrestrial laser scanning (TLS) technique applied as a monitoring technique to obtain the point cloud geometry of the Marcus Aurelius Exedra, thus, to produce a precise and reliable virtual model of the structure. The virtual model allows identifying more precisely the areas of the structure affected by displacements, although slight, obtained from the DInSAR analysis, that need further investigation. TLS technique can be considered as a useful tool to support and validate the information, and consequently its interpretation, acquired by both traditional and innovative monitoring systems, such as the DInSAR technique. In this work, on-site inspections were necessary for the surveying to cover and match all the areas of interest

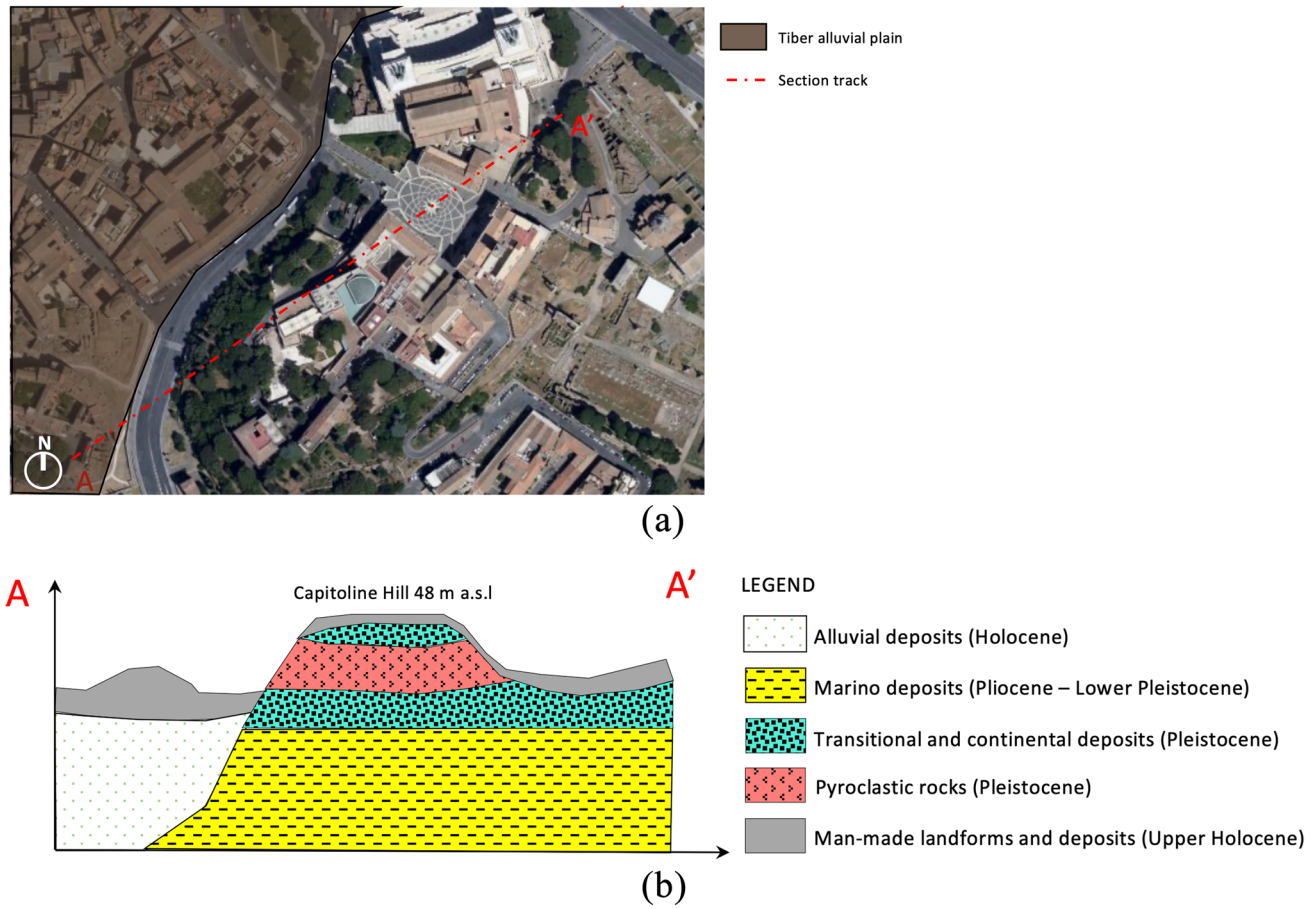

Fig. 9 Track of the geological section A–A′ (**a**) and geological cross section (**b**). Topography derived from the official stratigraphy provided by Isprambiente (https://www.isprambiente.gov.it/Media/carg/374 ROMA/Foglio.html)

and to highlight any critical aspects of the work. A survey area plan was sketched on paper to determine the location of scanner (Fig. 12).

It was to ensure that all the information and detail of the structure was covered. Indeed, the primary constraint for the data acquisition was the presence of furnishing and sculptures, which could have created gaps on the acquired surfaces. It used only one scanner to scan the whole survey area. Therefore, it has been necessary to move the scanner to different scan stations to check the entire site. As shown in Fig. 12, the TLS survey included scans collected from different positions distributed over the area of interest, functional to retrieve an overall point cloud reducing shadow areas. The leading surveying equipment used for the geometrical reconstruction of Marcus Aurelius Exedra was the Leica BLK360 laser scanner. The TLS was placed on a heavy tripod to reduce possible movements and torsions in the basement. The height of the tripod was set to approximately 1.2 m. The key technical specifications of the Leica BLK360 are listed in Table 4.

The instrument provides high-resolution scans with a performance range of 360,000 points/second, an integrated HDR camera that colorizes the scans, and a distance accuracy of up to ± 4 mm. The internal color camera can produce photorealistic 3D color scans (color overlay). The device provides a $360° \times 300°$ view range, capturing high-resolution scans up to 60 m from the station point. The generated point clouds and images were saved on the inserted SD memory card and, thus, can be easily transferred to another device. The scans were acquired consecutively and continuously to achieve the same external lighting conditions. The duration of each scan was approximately 10 min (the expected scan time is determined according to the selected resolutions, quality value, and scan range). Laser scanner surveys were arranged to detect the whole accessible area of the Marcus Aurelius Exedra in their external and internal parts. All assessments have been made related to the laser scanner features, the architectural structures, and the site accessibility. Data acquisitions were accurately planned to optimize the number, the positions, the resolution, and the field of view of the

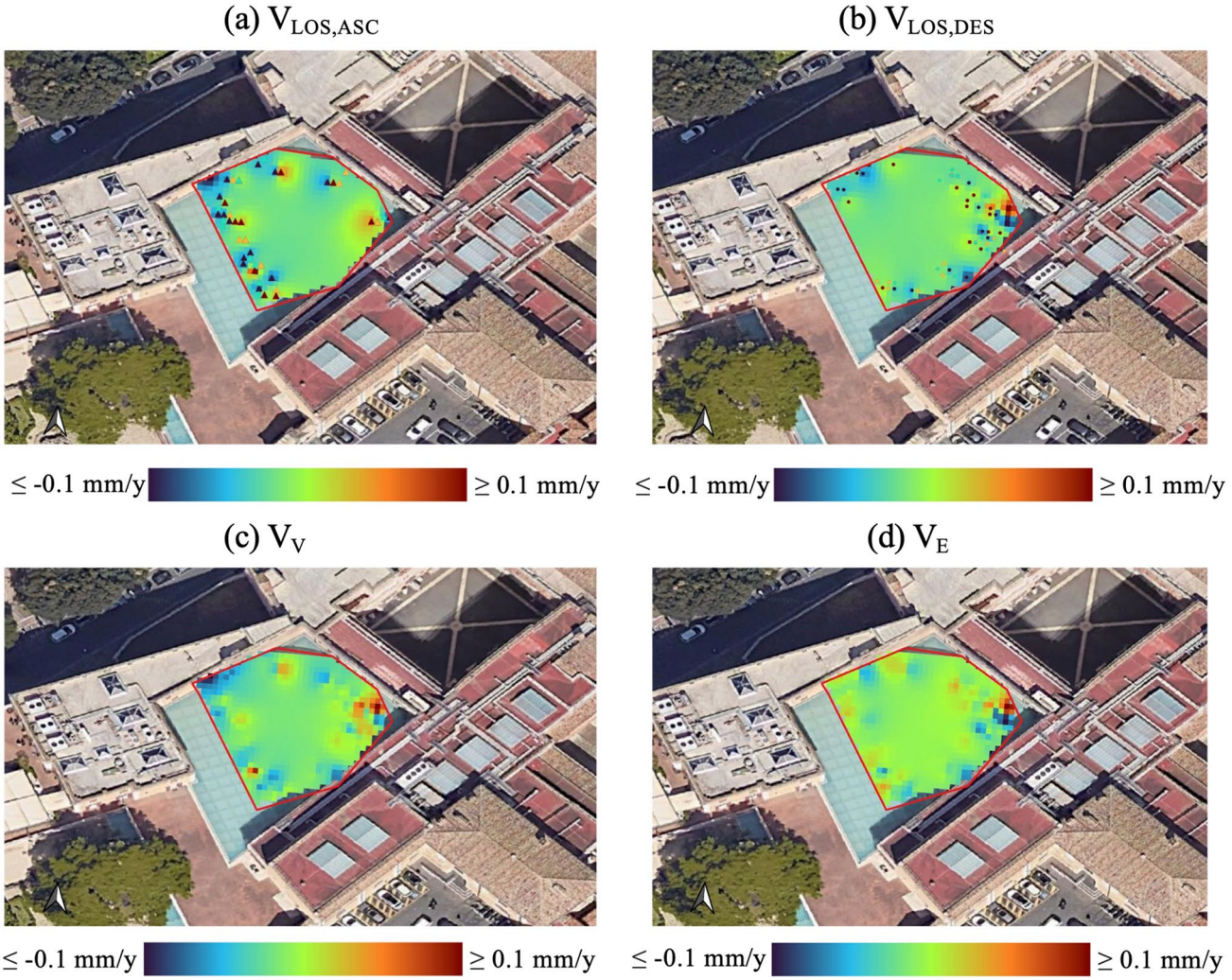

Fig. 10 Mean velocity maps of the Marcus Aurelius Exedra (local scale): ASC (**a**) and DES (**b**) data, with IDW interpolation; vertical (**c**) and E–W (**d**) components of the mean velocity

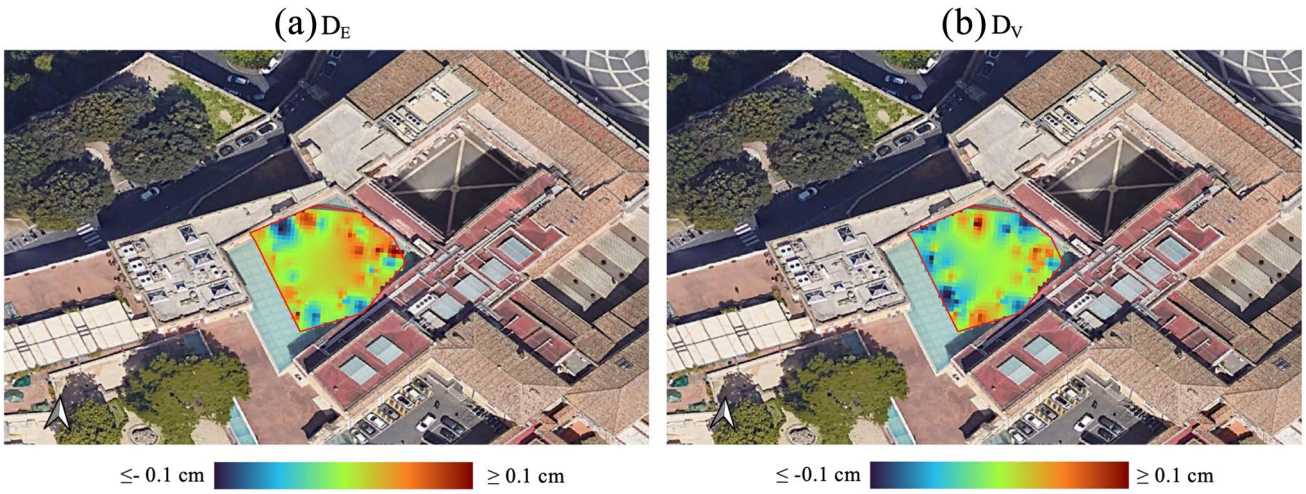

Fig. 11 Displacement maps of the Marcus Aurelius Exedra: E–W (**a**) and vertical (b) components of the displacement

Table 3 Summary of min and max vertical (VV) and horizontal (VE) velocities and vertical (DV) and horizontal (DE) displacements during 2012–2020—Marcus Aurelius Exedra

Value	V_V (mm/year)	V_E (mm/year)	Dv (cm)	D_E (cm)
Min (downwards/west)	−0.076	−0.417	−0.032	−2.147
Max (upwards/east)	0.208	0.361	1.196	0.928

Table 4 Technical specification of Leica BLK360

Scan parameters	Leika BLK360
Maximum range (m)	60 m
Minimum range (m)	0.6 m
Field of view (°)	360° (horizontal) × 360° (vertical)
Scanning speed	Up to 360,000 pts/s
Scan duration (min)	3 min
Ranging accuracy	4 mm @ 10 mm / 7 mm @ 20 mm
Internal memory	Storage for > 100 setup

scans. The acquired data that carried highly detailed spatial information were imported into Autodesk ReCap 360 software for further processing and point cloud visualization. Processing the TLS data included registering and filtering the 3D point clouds by eliminating noise, outliers, and undesired points. Later, raw cleaned data were imported directly from Autodesk ReCap to Autodesk Revit by Point Cloud Tool in *.rcp format, where an automatic optimization method, based on the Iterative Closest Point (ICP) algorithm, aligned, and registered the scans without any possible interventions by the operator. The resulting point cloud was made by more than 324 million points (distanced from each other by 3 mm on average). 3D point clouds are used in the BIM platform as a metric reference and reference plans tool to precisely identify the elements of the analyzed structure subjected to the vertical and horizontal displacements computed from SAR analysis. Figure 13 shows the raw point cloud model of the case study.

Fig. 12 Position of the laser scanner during data collection process at Sala del Giardino Romano (in blue) and Galleria del Muro Romano (in orange) (color figure online)

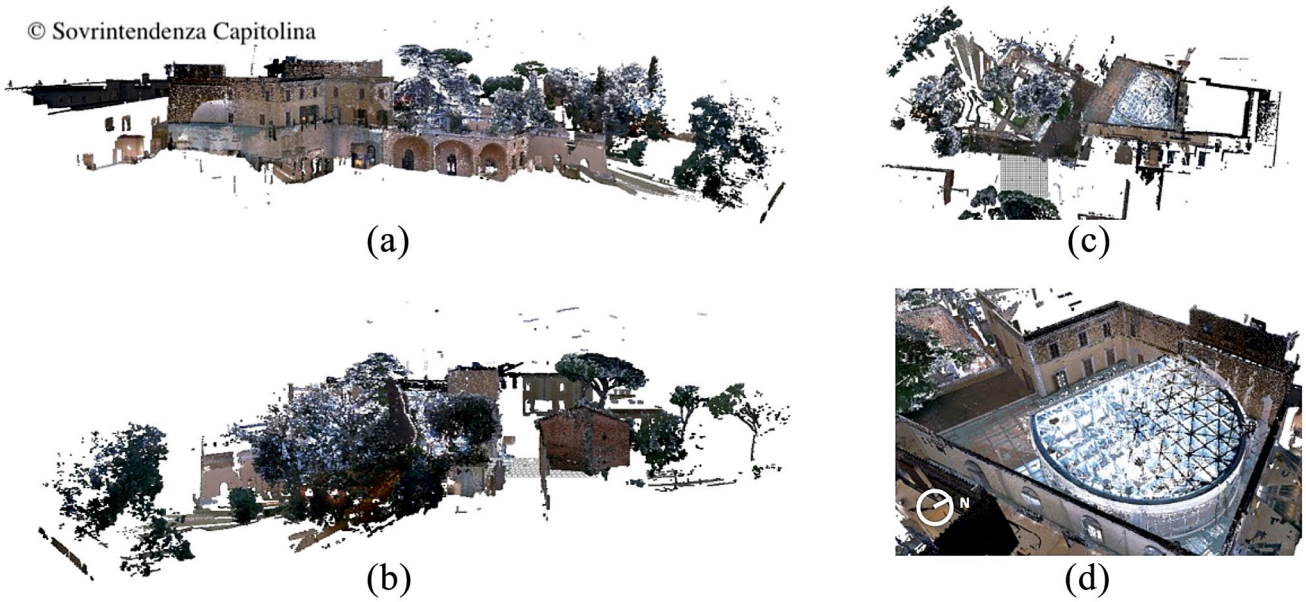

Fig. 13 Raw laser-scanned data of the Marcus Aurelius Exedra: external N–S (**a**) and S–N (**b**) view, top view with highlights of the roof (**c**, **d**)

4 Deformation assessment and discussion

In this section, the evaluation of construction deformations based on the combination of elaborated DInSAR results and on-site measurements is illustrated, according to the final step of the proposed flowchart illustrated in Fig. 1. Generally, the ground deformations captured by DInSAR technique at urban and building scales can be due to different causes, such as underground works, development of soil consolidation processes caused by changes in the soil loading conditions, landslides involving motions along both vertical and horizontal directions coupled with rotations, and extreme events. In this study, attention is given to the monitoring of ground settlements and the evaluation of their effects on the construction elements, by employing DInSAR measurements in terms of trend displacements of the deformation time series. The trend provides a qualitative information regarding the motion of the structure, which can help in the interpretation of the structural deformation evolution. This is done by combining on-site measurements and knowledge process for the construction with the elaborated SAR measurements. That is, the displacements' trend, i.e., the mean velocity and displacement in the considered time interval, can support the interpretation of the displacement evolution at a wide area and local scale, providing qualitative information about movement patterns to identify critical areas of buildings. The rationale behind the proposed combination is to use the 3D point cloud model geometric information with the DInSAR measures to localize better the critical areas, previously identified through the DInSAR measurements, of concern for the conservation of the building that need further and more in-depth investigations. In this sense, such preliminary information can be used to determine the structures more affected by the anomalies allowing a sensible inspection time reduction from the geometric identification phase. The laser-scanned data can support the assessment and interpretation of the satellite data since the point cloud replicates the real structure. Performing an intuitive analysis of the degree of fit between the point cloud and the displacement maps enable determining which part of the monitored structure is involved in the displacement phenomena described in the previous section and assigning structural attributes to the colored areas. An example of the proposed integration at the local scale is provided in Fig. 14, where the E–W displacement map of the Marcus Aurelius Exedra is compared to the point cloud model.

From the figure, it is possible to state that the blue-colored circles that are affected by displacements towards the West direction with a velocity of 0.417 mm/year (Fig. 14a) correspond to the six columns of the structure. Furthermore, the continuous displacement maps show vertical displacements in absolute value smaller than horizontal displacements. However, the maximum positive (upwards) and negative (downwards) displacements are localized in the six columns on the drum. Recognizing a particular trend on the columns through satellite information allows providing the precise location of the area to be inspected and monitored more in depth to take timely action to reduce risks. Moreover, the use of TLS technique in the field of deformation monitoring is related to scan the same point in different epochs, allowing a direct cloud-to-cloud comparison. In this case, point clouds can be used directly to detect changes between two clouds

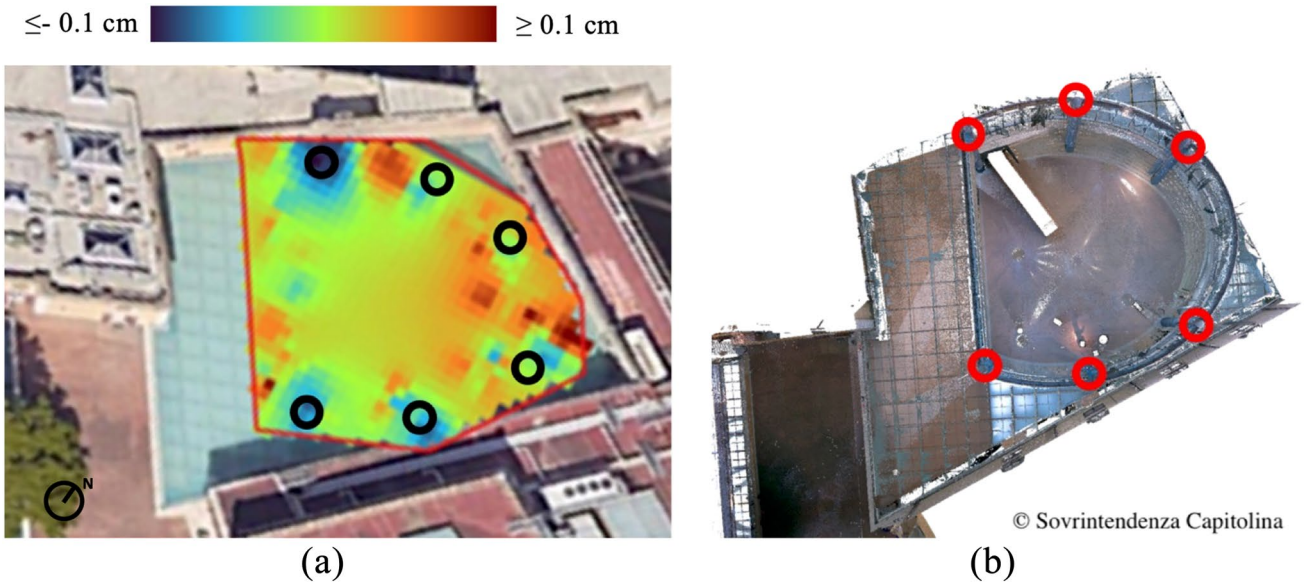

Fig. 14 Comparison between the E–W displacement map (**a**) and the point cloud of the Marcus Aurelius Exedra (**b**)

collected at other times by comparing the current situation (at time t_1) with the initial reference situation (at time t_0). To support the results carried out by the DInSAR analysis, it has been useful to compare the "*as-built*" model obtained from TLS that describes the current condition of the analyzed structure and the "*as-design*" model obtained from the original technical drawing. The comparison is depicted in Fig. 15, where the sections of the two models are purposely overlapped to highlight the difference in the vertical direction between the two epochs.

From the figure, on the right side of the roof (Fig. 15d), there is a downwards of the point cloud model of about − 0.03 m while, on the left side (Fig. 15c), the same model shows an upwards displacement (about 0.04 m) concerning the reference BIM model in red. Both models offer a differential altitude shift according to the displacement maps illustrated in Fig. 11b. Therefore, results confirm satellite data robustness when used as tool aiming at driving the TLS technology for monitoring displacements. Moreover, the time history measured by the DInSAR displacement near the section cut (green star of the Fig. 7a) shows an upward cumulative displacement over 1 cm that, considering the approximation of the satellite measurements, is in a good agreement with the TLS inspection. It is worth mentioning that, since the satellite measurements have found their mature applicability only in the last decade, the DInSAR displacement time series can cover only a certain period of the construction's overall lifetime and the cumulative displacements can be computed at the end of the observation interval to have an overall value to be compared with reference thresholds. More precisely, in the absence of information on the structure condition at the time zero of the satellite monitoring, it is only possible to state that if the cumulated differential displacement retrieved from DInSAR measurements exceeds the limit threshold, that damaged condition has been attained from the structure. Conversely, if some information is available on the damage condition of the structure at the time zero or before the beginning of the DInSAR time series, then the cumulative displacements related to the monitoring interval can be used more consciously to draw considerations on the evolution of structural damage during the monitored period [18]. A more reliable correlation between the expected and observed displacement, i.e., with a small degree of uncertainty, could occur when the acquisition of satellite radar images begins in corresponding with the construction operational life. The comparison between point cloud model and BIM show results in line with the trends visualized by the satellite data. The comparison in terms of magnitude shows a difference that could be considered reasonable due to the uncertainty in the positioning of the satellite measures (4 cm for TLS and 1 cm for DInSAR). However, such comparison is of relative importance since the real initial state is not known; therefore, it makes sense to carry out a comparison related to the direction and orientation of the displacement trends.

5 Conclusions

The spread of the advanced DInSAR techniques for generating spatially deformation time series has highly contributed to the development of applications aiming at the structural stability assessment of buildings and infrastructures. In this context, the primary support may derive from integrating

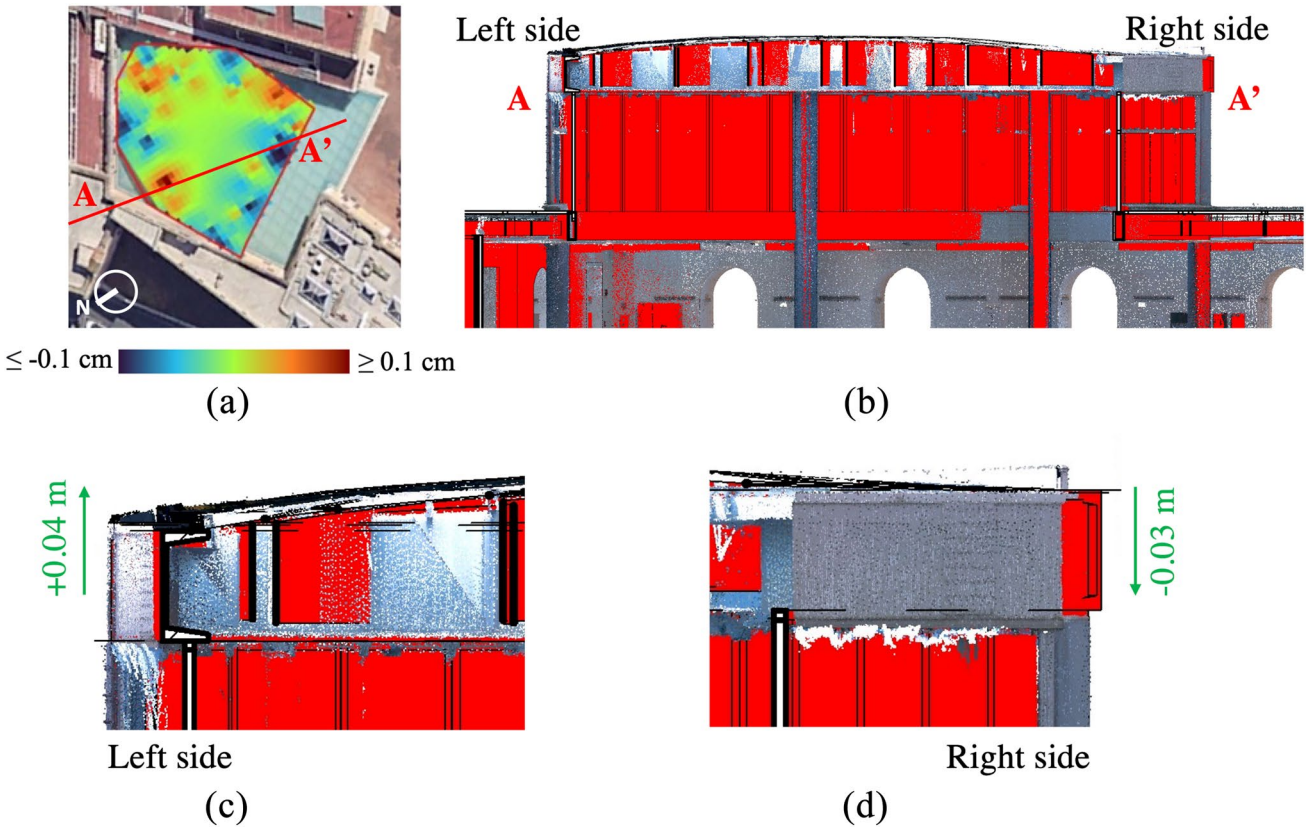

Fig. 15 Pointwise comparison: section cut and highlight of the upward displacement position shown in Fig. 7a (**a**) and section showing the overlap between the reference BIM model (colored in red) and 3D model obtained from TLS (**b**), zoom of the left (**c**) and right (**d**) side with indication of the raising (+0.04 m) and lowering (−0.03 m) in the left and right side, respectively, measured by TLS technology (color figure online)

DInSAR measurements and the 3D point cloud model retrieved from the TLS technique. In this work, a methodology jointly exploiting satellite DInSAR results, and a TLS-derived point cloud model has been proposed to identify possible displacement phenomena affecting built heritage. The proposed methodology is a preliminary tentative of combining the information coming from two different technologies: the traditional technology (TLS) and the innovative technology (DInSAR). Both provide different information that combined allow to make more robust the inspection process, especially in buildings or infrastructure that are difficult to be investigated. Indeed, while the DInSAR measurements allow to have the history of the displacements, even going back to different years, the TLS technology permits to go more in-depth in the geometrical description. The methodology has been applied to the CSK-based DInSAR time series relevant to the Capitoline Museums in Rome (Italy). The subsequent elaboration of the satellite data has led to obtain a picture of the deformation condition in the investigated period. Indeed, by analyzing the velocity trends and statistics of the PSs belonging to the studied building, deformation maps are retrieved to identify the critical area of the building to be further investigated. Exploiting satellite data, especially in the case of buildings placed in cultural heritage sites and constrained to the preservation of their countenance, can provide helpful information through time series analysis. Combining the displacement data derived from the DInSAR monitoring with the geometric information retrieved from the TLS survey was demonstrated as an interesting tool for spatial analysis of the structural stability of built heritage subjected to natural and man-made hazards, and consequently, for supporting preservation activities. Furthermore, the effectiveness of DInSAR techniques in analyzing deformation and displacement processes affecting cultural heritage, when supported by geological information, can help address adopting appropriate mitigation measures. Indeed, it is possible to understand if the examined structure is in a stable area or is subjected to settlements and the direction along which they are active. The main benefits of combining satellite data with on-site information are: (i) the availability of data covering a long period (usually over five years) obtained from DInSAR technique. Such type of data is only able to approximatively identify some anomalous trends (especially because their geometrical accuracy is not

very high) and (ii) the TLS technique allows to redesign the 3D point cloud (or better *driven*) to carry out a more in-depth investigation in the areas previously identified through the DInSAR measurements. In this sense, especially in a cultural heritage area, such preliminary information will allow to determine what are the structures more affected by anomalies. Finally, it can be concluded that the proposed methodology can be easily used for monitoring and identifying possible anomalous trends to be inspected more in-depth allowing a sensible inspection time reduction.

Acknowledgements The research project reported in this paper was conducted thanks to the financial support from DCP-ReLUIS 2021-2024 and was in part sponsored by the NATO Science for Peace and Security Programme under grant id. G5924.Morevover, was part of ERIS Project supported by LAZIO INNOVA (n. G09493—PO FESR LAZIO 2014/2020). The authors are gratefully acknowledged to the Capitoline Museums of Rome.

Declarations

Conflict of interest The author(s) declared no potential conflicts of interest with respect to the research, authorship, and/or publication of this article.

References

1. Potenza F et al (2015) Long-term structural monitoring of the damaged Basilica S. Maria di Collemaggio through a low-cost wireless sensor network. J Civ Struct Health Monit 5:655–676
2. Crognale M, Potenza F, Gattulli V (2023) Fatigue damage identification by a global-local integrated procedure for truss-like steel bridges. Struct Control Health Monitor 2023:1–23
3. Domaneschi M et al (2021) Laboratory investigation of digital image correlation techniques for structural assessment. In: Yokota H, Frangopol DM (eds) Bridge maintenance, safety, management, life-cycle sustainability and innovations. CRC Press, pp 3260–3266
4. Forster B (1985) An examination of some problems and solutions in monitoring urban areas from satellite platforms. Int J Remote Sens 6(1):139–151
5. Zhu M et al (2018) Detection of building and infrastructure instabilities by automatic spatiotemporal analysis of satellite SAR interferometry measurements. Remote Sens 10(11):1816
6. Giordano PF et al (2022) Damage detection on a historic iron bridge using satellite DInSAR data. Struct Health Monit 21(5):2291–2311
7. Gabriel AK, Goldstein RM, Zebker HA (1989) Mapping small elevation changes over large areas: differential radar interferometry. J Geophys Res Solid Earth 94(B7):9183–9191
8. Massonnet D, Feigl KL (1998) Radar interferometry and its application to changes in the Earth's surface. Rev Geophys 36(4):441–500
9. Rosen PA et al (2000) Synthetic aperture radar interferometry. Proc IEEE 88(3):333–382
10. Ciampalini A et al (2014) Analysis of building deformation in landslide area using multisensor PSInSAR™ technique. Int J Appl Earth Obs Geoinf 33:166–180
11. Confuorto P et al (2019) Monitoring of remedial works performance on landslide-affected areas through ground-and satellite-based techniques. CATENA 178:77–89
12. Reale D et al (2011) Tomographic imaging and monitoring of buildings with very high resolution SAR data. IEEE Geosci Remote Sens Lett 8(4):661–665
13. De Canio G et al (2015) Seismic monitoring of the cathedral of Orvieto: combining satellite InSAR with in-situ techniques. In: Proceedings of the 7th international conference on structural health monitoring of intelligent infrastructure, Torino, Italy
14. De Falco A, Resta C, Squeglia N (2022) Satellite and on-site monitoring of subsidence for heritage preservation: a critical comparison from Piazza del Duomo in Pisa, Italy. In: Lancellotta R, Viggiani C, Flora A, de Silva F, Mele L (eds) Geotechnical engineering for the preservation of monuments and historic sites III. CRC Press, pp 548–559
15. Del Soldato M et al (2018) Multisource data integration to investigate one century of evolution for the Agnone landslide (Molise, southern Italy). Landslides 15:2113–2128
16. Di Martire D et al (2016) Landslide detection integrated system (LaDIS) based on in-situ and satellite SAR interferometry measurements. CATENA 137:406–421
17. Mazzanti P, Cipriani I (2011) Terrestrial SAR interferometry monitoring of a civil building in the city of Rome. In: FRINGE 2011'Workshop on ERS/Envisat SAR Interferometry,'FRINGE11', Frascati, Italy
18. Di Carlo F et al (2021) On the integration of multi-temporal synthetic aperture radar interferometry products and historical surveys data for buildings structural monitoring. J Civ Struct Health Monit 11(5):1429–1447
19. Mele A et al (2022) On the joint exploitation of satellite DInSAR measurements and DBSCAN-Based techniques for preliminary identification and ranking of critical constructions in a built environment. Remote Sens 14(8):1872
20. Bozzano F et al (2020) Satellite A-DInSAR monitoring of the Vittoriano monument (Rome, Italy): implications for heritage preservation. Ital J Eng Geol Environ 2:5–17
21. Talledo DA et al (2022) Satellite radar interferometry: potential and limitations for structural assessment and monitoring. J Build Eng 46:103756
22. Arangio S et al (2014) An application of the SBAS-DInSAR technique for the assessment of structural damage in the city of Rome. Struct Infrastruct Eng 10(11):1469–1483
23. Bonano M et al (2012) Long-term ERS/ENVISAT deformation time-series generation at full spatial resolution via the extended SBAS technique. Int J Remote Sens 33(15):4756–4783
24. Bayramov E et al (2022) Quantitative assessment of ground deformation risks, controlling factors and movement trends for onshore petroleum and gas industry using satellite Radar remote sensing and spatial statistics. Georisk Assess Manag Risk Eng Syst Geohazards 16(2):283–300
25. Pärn EA, Edwards DJ (2017) Conceptualising the FinDD API plug-in: a study of BIM-FM integration. Autom Constr 80:11–21
26. Barazzetti L et al (2015) Cloud-to-BIM-to-FEM: structural simulation with accurate historic BIM from laser scans. Simul Model Pract Theory 57:71–87
27. Díaz Vilariño L et al (2018) Scan planning and route optimization for control of execution of as-designed BIM. ISPRS Int Arch Photogramm Remote Sens Spat Inf Sci. https://doi.org/10.5194/isprs-archives-XLII-4-143-2018
28. Tan K et al (2020) Estimation of soil surface water contents for intertidal mudflats using a near-infrared long-range terrestrial laser scanner. ISPRS J Photogramm Remote Sens 159:129–139
29. Philipp MB, Levick SR (2019) Exploring the potential of C-Band SAR in contributing to burn severity mapping in tropical savanna. Remote Sens 12(1):49
30. Kaasalainen S et al (2010) Comparison of terrestrial laser scanner and synthetic aperture radar data in the study of forest defoliation. na

31. Odipo VO et al (2016) Assessment of aboveground woody biomass dynamics using terrestrial laser scanner and L-band ALOS PALSAR data in South African Savanna. Forests 7(12):294
32. Berardino P et al (2002) A new algorithm for surface deformation monitoring based on small baseline differential SAR interferograms. IEEE Trans Geosci Remote Sens 40(11):2375–2383
33. Lanari R et al (2004) A small-baseline approach for investigating deformations on full-resolution differential SAR interferograms. IEEE Trans Geosci Remote Sens 42(7):1377–1386
34. Zebker HA, Villasenor J (1992) Decorrelation in interferometric radar echoes. IEEE Trans Geosci Remote Sens 30(5):950–959
35. Manunta M et al (2008) Two-scale surface deformation analysis using the SBAS-DInSAR technique: a case study of the city of Rome, Italy. Int J Remote Sens 29(6):1665–1684
36. Casu F, Manzo M, Lanari R (2006) A quantitative assessment of the SBAS algorithm performance for surface deformation retrieval from DInSAR data. Remote Sens Environ 102(3–4):195–210
37. Manunta M et al (2019) The parallel SBAS approach for Sentinel-1 interferometric wide swath deformation time-series generation: algorithm description and products quality assessment. IEEE Trans Geosci Remote Sens 57(9):6259–6281
38. Wang G, Gertner G, Anderson AB (2005) Sampling design and uncertainty based on spatial variability of spectral variables for mapping vegetation cover. Int J Remote Sens 26(15):3255–3274
39. Kruse FA et al (2012) Mapping alteration minerals at prospect, outcrop and drill core scales using imaging spectrometry. Int J Remote Sens 33(6):1780–1798
40. Burrough PA (1986) Principles of geographical. Information systems for land resource assessment. Clarendon Press, Oxford
41. Schut G (1976) Review of interpolation methods for digital terrain models. Can Surveyor 30(5):389–412
42. Panella R, Tugnoli ML (2015) The extension of Rome's Capitoline Museums and the design of a new Hall on the site of the ancient 'Giardino Romano.' Front Archit Res 4(3):171–185
43. Stramondo S et al (2008) Subsidence induced by urbanisation in the city of Rome detected by advanced InSAR technique and geotechnical investigations. Remote Sens Environ 112(6):3160–3172
44. Tapete D et al (2012) Satellite radar interferometry for monitoring and early-stage warning of structural instability in archaeological sites. J Geophys Eng 9(4):S10–S25